Supplement of Biogeosciences, 17, 2853–2874, 2020
https://doi.org/10.5194/bg-17-2853-2020-supplement

Biogeosciences Open Access EGU

Supplement of

Comparison of eddy covariance CO_2 and CH_4 fluxes from mined and recently rewetted sections in a northwestern German cutover bog

David Holl et al.

Correspondence to: David Holl (david.holl@uni-hamburg.de)

1 Gap-filling methods from literature

Table S1. Overview of methods applied in literature to gap-fill eddy covariance methane flux time series.

Method		References
Interpolation		Hanis et al. (2013); Dengel et al. (2011)
Averaging		Hatala et al. (2012); Mikhaylov et al. (2015)
Arrhenius-type non-linear functions	half-hourly	Kroon et al. (2010); Forbrich et al. (2011); Hommeltenberg et al. (2014); Goodrich et al. (2015)
	downsampled	Suyker et al. (1996); Friborg and Christensen (2000); Rinne et al. (2007); Long et al. (2010); Wille et al. (2008); Jackowicz-Korczyński et al. (2010); Parmentier et al. (2011); Brown et al. (2014); Shoemaker et al. (2015); Mikhaylov et al. (2015)
Look-up tables		Pypker et al. (2013); Hommeltenberg et al. (2014); Bhattacharyya et al. (2014)
Mean diurnal variation		Dengel et al. (2011); Jha et al. (2014)
Marginal distribution sampling		Alberto et al. (2014); Shoemaker et al. (2015)
Machine learning	Artificial neural networks	Dengel et al. (2013); Deshmukh et al. (2014); Knox et al. (2015); Goodrich et al. (2015); Nemitz et al. (2018); Knox et al. (2019); Kim et al. (2019)
	Support vector machines	Kim et al. (2019)
	Random forest	Kim et al. (2019)

2 Model setup and input selection scheme

This section describes the selection of model inputs (see Table A1) using our scoring table approach. Also, the method we used to select properties for the multilayer perceptron (MLP) neural networks is outlined. The MLPs were set up with one hidden layer, tan-sigmoid activation functions, a single output layer node with a linear transfer function and Levenberg-Marquardt backpropagation as supervised learning method. See Papale and Valentini (2003), Dengel et al. (2013), Sarle (1994) for details on MLP architecture. The input data was divided randomly in 70 % training and 30 % validation data. Inputs were re-scaled before training to range between -1 and 1. Training data were used to optimize the network weights and biases for low MSE. Validation data served as inputs independent from training data to check the generalization capability of the model. The model

performance in relation to the validation data was used to avoid overfitting by terminating the learning process if for six consecutive iterations the MSE of the validation data did not decrease (early stopping). Instead of using the response of a single MLP, we calculated the ensemble average of multiple networks starting with varying initial weights and different sets of training and validation data each. This method is frequently described in neural network literature (Naftaly et al., 1997; Perrone and Cooper, 1993; Wolpert, 1992; Hashem, 1997; Haykin, 1999) as one type of so called committee machines. To avoid unnecessarily complex network architecture and thereby a higher amount of model parameters we inspected the model performance of committee machines with 100 MLPs each for different numbers of hidden layer nodes (#HLN) between 1 and 20. We expected to find a #HLN optimum at the AIC minimum. However, for different gases and data sets, we encountered two functional forms a relation like this would commonly assume. A parabola-like curve with a clear minimum and an asymptotic function of the form $AIC(\#HLN) = \#HLN^{-1} + a$. We fitted parabolas to the according data sets and assumed the function vertex as #HLN optimum. In the other cases, we fitted reciprocal functions and differentiated the results. We rounded the first derivatives to the nearest multiple of 10 in case of CH_4 and to 100 in case of CO_2 flux modeling. We then defined the #HLN optimum to be at the position where the rounded derivative turns zero for the first time. We performed #HLN optimization in each case before applying MLPs for input sensitivity analysis or gap-filling.

We applied a selection procedure aiming for the identification of redundant as well as irrelevant model inputs. This scheme evaluates the outcome of stepwise MLRs in combination with the analysis of the response of MLPs to differently manipulated versions of the input space. We used methods addressing predictive and causal importance as defined by Sarle (1997). In short, predictive importance measures are those that check the change of model performance when an input is omitted, whereas causal importance measures evaluate the change of a performance function when inputs are manipulated. The latter can be realized by degrading the variability of an input for example by replacing it partly with its average (as in Schmidt et al., 2008; Hunter et al., 2000). Three categories of potential model inputs were presented to the selection scheme. Thirty minute time series of meteorological and soil (Biomet) variables, fuzzy variables representing diurnal and seasonal cycles (following Papale and Valentini, 2003) and footprint variables in the form of surface class contribution estimates. Table A1 gives an overview of the available variables. Note that in Year 1 no soil properties were recorded.

We derived a second set of Biomet variables by estimating the time lag between each Biomet variable and the gas flux time series and subsequently shifting each Biomet time series by the calculated time lag. We used the lag time within a one-day window for which the absolute cross-correlation between Biomet and gas flux time series was maximized (Kettunen et al., 1996) to shift the respective Biomet time series.

Three data sets were used for sensitivity analysis: Only the original Biomet data, only the lagged data and both. All data sets were extended by fuzzy and footprint data. We applied four methods to estimate the relevance of the individual inputs and combined them via a scoring table. If an input was selected by one method, one point was assigned to it. Inputs with more points were regarded as more important.

As previously applied by Dengel et al. (2013) for EC flux gap-filling, we used the outcome of a stepwise multilinear regression (MLR) with bidirectional elimination to identify important model inputs. Independent variables that remained in the final model received one point in our scoring table. The calculations were made using the Matlab 8.4 Statistics and Machine

Learning Toolbox following Draper and Smith (1998). At each step the p-values of an F-statistic of models with or without each input were evaluated by comparing them with an enter condition $p_{enter} = 0.05$ and an exit condition $p_{remove} = 0.1$. If inputs currently not in the model had p-values below p_{enter}, the one with the lowest value was included into the model until the next step (forward selection). If inputs currently in the model had p-values above p_{remove}, the one with the highest value was removed from the model (backward elimination). These steps were repeated until the model could not be improved further by a single step. The initial model contained no inputs.

Following Schmidt et al. (2008), we calculated two similar measures of causal importance from the output of MLP ensembles. The variability of each input variable was manipulated by replacing 50 % and 100 % with its median, while all remaining variables in the input matrix were left unchanged. A MLP ensemble was first trained with the original data and then simulated with the artificial input matrix. The relation of the resultant mean squared errors (MSEs) was calculated and called relative error (RE). This process was repeated 1000 times for all input variables to obtain diverse results for different data divisions. The resulting values for RE were binned into six classes with centers at 0.8, 0.9, 1.0, 1.1, 1.2 and 1.3. If the latter was the bin with the most counts, one point was assigned to this input variable in the scoring table, meaning that the manipulation of this input vector resulted in a deterioration of the respective MSE of more than 25 % in most cases. This method yielded two measures of causal importance for each input variable, RE_{50} and RE_{100}, referring to the two percentages of data being manipulated.

We furthermore analyzed the weights resulting from MLP optimization based on the algorithm of Garson (1991) as presented in Olden and Jackson (2002). This method interprets the weights of a neural network similar to the coefficients of a linear model. Before calculating the relative importance (RI) of an input, the products of the weights that connect this input with each hidden neuron and the output layer is determined and normalized by the sum of weight products feeding also into the same hidden unit. These so called neuron contributions are summed up and normalized by the sum of all neuron contributions resulting in the RIs of all inputs. We calculated the mean, median and maximum RIs of 1000 MLP runs for all input variables. We then compiled three lists in which we sorted the inputs in descending order with respect to the determined statistics. The lengths of those lists were afterwards shortened to equal the number of variables that were included in the MLR model that was derived before – only variables with the highest RI statistics stayed in the lists. All inputs that occurred at least in two of three lists received one point in the scoring table, which was completed with this step. We then summed up the scores for all input variables and calculated two score thresholds above which an input was to be selected. One threshold was derived for the original and the lagged Biomet variables, one for fuzzy and footprint data. We proceeded like this owing to the structure of the three input data sets. Each Biomet variable occurred in two of three data sets, each fuzzy and footprint variable was part of all data sets, making it more likely for them to reach a high score. We calculated the mean score of the respective variable category and used the next larger integer as a score threshold. The inputs that were selected via the scoring table were fed into a final stepwise MLR removing further apparently irrelevant model inputs. In the last step of the input selection algorithm we checked if both a variable and its lagged derivative remained in the input matrix. If so, the scores of those two variables were compared, and only the higher scoring variable stayed in the input matrix. In case there was no score difference, the lagged derivative was removed from the input space, whose reduction was hereby finished.

3 Model input selection results

To gain first insight into the relations between input variables and landscape-scale gas fluxes (tower view time series, TVTS) as well as between the input variables among each other, scatter plots were inspected and Pearson's correlation coefficient (r) was determined for each pair. See Table A1 for definitions of the quantity symbols used hereafter. Three Biomet time series correlate with r values of 0.4 or higher with CH_4 flux in both years: Lw_{out}, T_{air} and R_g. In Year 1, this list is extended by VPD and PAR while the highest linear relation exists with CC_{rew} (0.5) and $CC_{veg,\,rew}$ (0.6). In Year 2, additional connections with r values of 0.4 or higher include soil temperatures T_{Soil20}, T_{Soil2} and T_{Soil40}. Footprint variables were not as closely related as in Year 1. Nevertheless, $CC_{veg,\,rew}$ yields again the highest correlation among the footprint variables. Compared to F_{CH4}, linear relations between model input variables and CO_2 flux are more clear as the only strong connections exist with PAR and R_g (both r = 0.5 in Year 1 and r = 0.6 in Year 2). Regarding linear dependencies between Biomet variables, R_g and PAR (r > 0.9 both years), T_{air} and VPD (r = 0.7 in both years) as well as T_{air} and Lw_{out} (r > 0.9 both years) were highly correlated. In Year 2, soil temperatures were closely connected among each other (r > 0.9) and with T_{air} (r > 0.7). Water table depth was correlated negatively with all redox measurements at different positions in the soil profile, with the largest absolute r of -0.7 for the relation with $Redox_{20}$. WT was also correlated with T_{Soil20} (r = 0.3). The seasonality embedded in soil temperature measurements was reflected by high correlation coefficients with the two low-frequency fuzzy variables fuzzy variable summer ($fuzzy_{su}$) and fuzzy variable winter ($fuzzy_{wi}$). The deeper in the soil profile the temperature measurements were taken, the less amplitude response they show to diurnal variations and the less noisy the relation to the fuzzy data appears to be.

Correlation analysis emphasizes the (not surprising) fact that collinearity does exist in the model input space. In order to avoid overfitting and thereby to increase the predictive power of the applied models, we reduced the input matrices which drive these models using our scoring table approach. Results of this input variables selection are detailed in tables S2 to S5. As a measure to ascertain collinearity reduction, we calculated the condition numbers (Belsley et al., 2005) of the input matrices at successive stages of the selection process as well as for the complete original and time-lagged input series (see figures S1 and S2). Within all 12 data sets, the condition numbers dropped throughout the selection process by at least one order of magnitude denoting a consistent removal of collinear variables from the input space. In all cases, between 30 % and 40 % of the variables presented to the selection scheme were included in the final model input matrices.

In the following section, detailed results of our model input selection scheme are shown. The four tables cover two gases and two years. Within each table, results for the two land use types (surface class *drained*, SC_{dra} and surface class *rewetted*, SC_{rew}) are shown. See Table A1 for declarations of the used quantity symbols. Only variables reaching a score above the respective score threshold are included. Variables which were selected in the last step of the scheme and used for gas flux modeling are printed in bold face.

Table S2. Result of the model input selection scheme for Year 1 CO_2 fluxes. Score threshold for Biomet variables: SC_{dra} (6), SC_{rew} (6). Score threshold for Fuzzy & Footprint variables: SC_{dra} (9), SC_{rew} (10)

	Surface class *drained*		Surface class *rewetted*	
	Variable	Score	Variable	Score
Biomet	**Lw_{out}**	8	**Lw_{out}**	8
	T_{air}	8	**T_{air}**	8
	R_g	7	**R_g**	8
	PAR	7	Lw_{out}, lagged	8
	Lw_{out}, lagged	7	PAR	7
	R_g, lagged	7	VPD, lagged	6
	T_{air}, lagged	7	T_{air}, lagged	6
Fuzzy & Footprint	**$CC_{veg,\ dra}$**	12	**$CC_{veg,\ rew}$**	12
	$fuzzy_{su}$	12	**$fuzzy_{wi}$**	12
	$fuzzy_{wi}$	12	**$fuzzy_{af}$**	11
	$fuzzy_{af}$	9	**$fuzzy_{ni}$**	11
	$fuzzy_{ev}$	9	**$fuzzy_{mo}$**	10

Table S3. Result of the model input selection scheme for Year 2 CO_2 fluxes. Score threshold for Biomet variables: SC_{dra} (6), SC_{rew} (6). Score threshold for Fuzzy & Footprint variables: SC_{dra} (9), SC_{rew} (9)

	Drained		Rewetted	
	Variable	Score	Variable	Score
Biomet	**T_{air}**	8	**T_{air}**	8
	PAR, lagged	8	**T_{Soil2}**	8
	T_{Soil2}	7	**T_{Soil5}**	8
	$Redox_5$	7	**T_{Soil10}**	8
	T_{air}, lagged	7	**PAR, lagged**	8
	T_{Soil20}, lagged	7	**T_{Soil40}**	7
	$Redox_2$, lagged	7	T_{Soil40}, lagged	7
	T_{Soil5}	6	T_{Soil2}, lagged	7
	T_{Soil10}	6	T_{Soil5}, lagged	7
	$Redox_{10}$	6	T_{Soil10}, lagged	7
	$Redox_{20}$	6	**T_{Soil20}, lagged**	7
	WT, lagged	6	T_{Soil20}	6
	T_{Soil2}, lagged	6	**$Redox_2$**	6
	T_{Soil10}, lagged	6	**$Redox_{10}$**	6
	$Redox_5$, lagged	6	T_{air}, lagged	6
	$Redox_{10}$, lagged	6	$Redox_{20}$, lagged	6
	$Redox_{20}$, lagged	6		
Fuzzy & Footprint	**$CC_{veg,\ dra}$**	12	**$fuzzy_{su}$**	11
	$fuzzy_{wi}$	9	**$fuzzy_{wi}$**	11
	$fuzzy_{af}$	9	**$CC_{veg,\ rew}$**	9
	$fuzzy_{ev}$	9	**$fuzzy_{af}$**	9
	$fuzzy_{ni}$	9	**$fuzzy_{ev}$**	9
	$fuzzy_{su}$	9	**$fuzzy_{ni}$**	9

Table S4. Result of the model input selection scheme for Year 1 CH_4 fluxes. Score threshold for Biomet variables: SC_{dra} (6), SC_{rew} (6). Score threshold for Fuzzy & Footprint variables: SC_{dra} (8), SC_{rew} (8)

	Drained		Rewetted	
	Variable	Score	Variable	Score
Biomet	**VPD**	8	**VPD**	8
	T_{air}, lagged	8	Lw_{out}, lagged	8
	Lw_{out}	7	T_{air}, lagged	8
	T_{air}	7	**Lw_{out}**	7
	VPD, lagged	7	**p_{air}**	7
	Lw_{out}, lagged	6	**T_{air}**	7
Fuzzy & Footprint	**$CC_{veg, dra}$**	12	**$CC_{veg, rew}$**	12
	$fuzzy_{su}$	12	**$fuzzy_{su}$**	12
	$fuzzy_{af}$	10	**$fuzzy_{af}$**	11
	$fuzzy_{mo}$	8	**$fuzzy_{mo}$**	8
	$fuzzy_{wi}$	8		

Table S5. Result of the model input selection scheme for Year 2 CH_4 fluxes. Score threshold for Biomet variables: SC_{dra} (6), SC_{rew} (7). Score threshold for Fuzzy & Footprint variables: SC_{dra} (8), SC_{rew} (9)

	Drained		Rewetted	
	Variable	Score	Variable	Score
Biomet	**VPD**	8	**VPD**	8
	T_{Soil40}	8	WT	8
	T_{Soil5}	8	**T_{Soil5}**	8
	$Redox_{10}$	8	**T_{Soil20}**	8
	T_{Soil40}, lagged	8	**$Redox_{10}$**	8
	T_{Soil10}, lagged	8	**$Redox_{20}$**	8
	$Redox_5$, lagged	8	WT, lagged	8
	Lw_{out}	7	**$Redox_2$, lagged**	8
	T_{Soil2}	7	**T_{Soil40}**	7
	T_{Soil10}	7	T_{Soil2}	7
	$Redox_2$	7	T_{Soil40},lagged	7
	T_{Soil2}, lagged	7	**T_{Soil2},lagged**	7
	T_{Soil5}, lagged	7	T_{Soil5},lagged	7
	T_{Soil20}, lagged	7	T_{Soil5},lagged	7
	$Redox_2$, lagged	7	$Redox_{20}$, lagged	7
	$Redox_{10}$, lagged	7		
	T_{air}, lagged	6		
	T_{Soil20}	6		
	$Redox_{20}$	6		
	VPD, lagged	6		
	WT, lagged	6		
	$Redox_{20}$, lagged	6		
Fuzzy & Footprint	**$CC_{veg,\ dra}$**	12	**$CC_{veg,\ rew}$**	12
	$fuzzy_{su}$	10	**$fuzzy_{wi}$**	12
	$fuzzy_{mo}$	9	**$fuzzy_{mo}$**	9
	$fuzzy_{af}$	8	**$fuzzy_{su}$**	9

4 Effect of dimension reduction of model input space on matrix condition

In this section, matrix condition numbers of the differently manipulated versions of input variable combinations that were fed into the input selection scheme (first three groups from the left in the plots below) and condition numbers of matrices at the two final stages of the selection scheme (last two groups from the left in the plots below) are given. Lower condition numbers denote a smaller degree of linear dependencies within different variables in a matrix. Three data sets were modeled for each gas flux time series per year: The originally measured EC fluxes (tower view) representing landscape-scale integrated fluxes and the extracted time series, using EC footprint modeling, which relate to areas under different land use (drainage and rewetting) are shown.

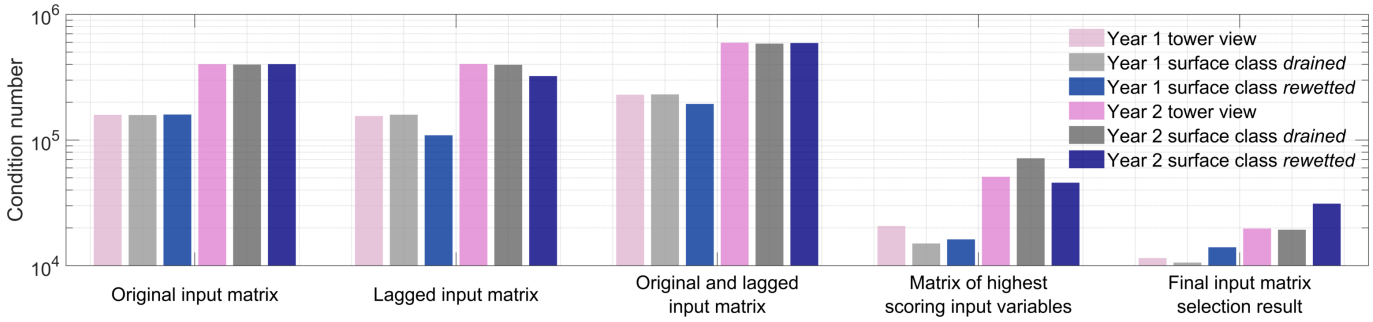

Figure S1. Matrix condition numbers of input combinations which were fed into the CH_4 flux model input selection scheme (first three groups from the left) and condition numbers of matrices at the two final stages of the selection scheme (last two groups from the left).

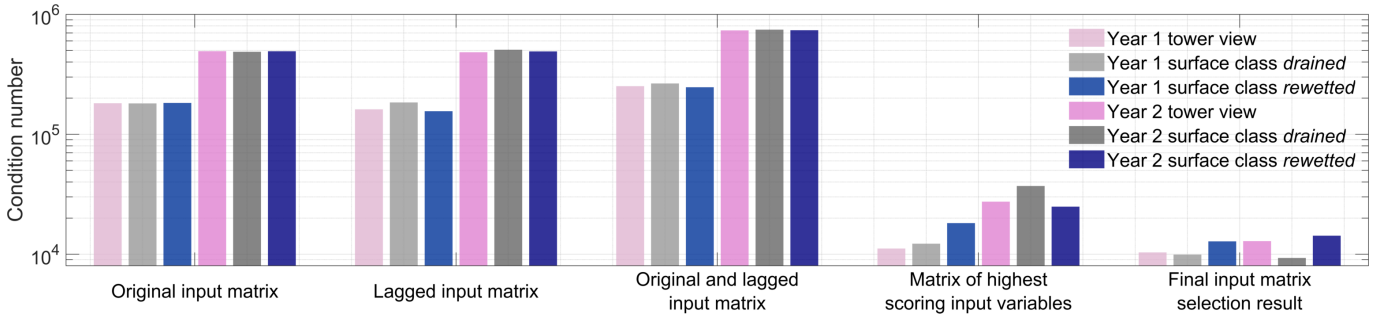

Figure S2. Matrix condition numbers of input combinations which were fed into the CO_2 flux model input selection scheme (first three groups from the left) and condition numbers of matrices at the two final stages of the selection scheme (last two groups from the left).

References

Alberto, M. C. R., Wassmann, R., Buresh, R. J., Quilty, J. R., Correa, T. Q., Sandro, J. M., and Centeno, C. A. R.: Measuring methane flux from irrigated rice fields by eddy covariance method using open-path gas analyzer, Field Crops Research, 160, 12 – 21, https://doi.org/10.1016/j.fcr.2014.02.008, 2014.

Belsley, D. A., Kuh, E., and Welsch, R. E.: Detecting and Assessing Collinearity, chap. 3, pp. 85–191, John Wiley & Sons, Ltd, https://doi.org/10.1002/0471725153.ch3, 2005.

Bhattacharyya, P., Neogi, S., Roy, K., Dash, P., a.K. Nayak, and Mohapatra, T.: Tropical low land rice ecosystem is a net carbon sink, Agriculture, Ecosystems & Environment, 189, 127 – 135, https://doi.org/10.1016/j.agee.2014.03.013, 2014.

Brown, M. G., Humphreys, E. R., Moore, T. R., Roulet, N. T., and Lafleur, P. M.: Evidence for a nonmonotonic relationship between ecosystem-scale peatland methane emissions and water table depth, Journal of Geophysical Research - Biogeosciences, 119, 826 – 835, https://doi.org/10.1002/2013JG002576, 2014.

Dengel, S., Levy, P. E., Grace, J., Jones, S. K., and Skiba, U. M.: Methane emissions from sheep pasture, measured with an open-path eddy covariance system, Global Change Biology, 17, 3524 – 3533, https://doi.org/10.1111/j.1365-2486.2011.02466.x, 2011.

Dengel, S., Zona, D., Sachs, T., Aurela, M., Jammet, M., Parmentier, F. J. W., Oechel, W., and Vesala, T.: Testing the applicability of neural networks as a gap-filling method using CH_4 flux data from high latitude wetlands, Biogeosciences, 10, 8185 – 8200, https://doi.org/10.5194/bg-10-8185-2013, 2013.

Deshmukh, C., Serça, D., Delon, C., Tardif, R., Demarty, M., Jarnot, C., Meyerfeld, Y., Chanudet, V., Guédant, P., Rode, W., Descloux, S., and Guérin, F.: Physical controls on CH_4 emissions from a newly flooded subtropical freshwater hydroelectric reservoir: Nam Theun 2, Biogeosciences, 11, 4251–4269, 2014.

Draper, N. R. and Smith, H.: Applied Regression Analysis, John Wiley and Sons, New York, 3rd edn., https://doi.org/10.1198/tech.2005.s303, 1998.

Forbrich, I., Kutzbach, L., Wille, C., Becker, T., Wu, J., and Wilmking, M.: Cross-evaluation of measurements of peatland methane emissions on microform and ecosystem scales using high-resolution landcover classification and source weight modelling, Agricultural and Forest Meteorology, 151, 864 – 874, https://doi.org/10.1016/j.agrformet.2011.02.006, 2011.

Friborg, T. and Christensen, T.: Trace gas exchange in a high-arctic valley 2 . Landscape CH 4 fluxes measured and modeled using eddy correlation have measurements, Global Biogeochemical Cycles, 14, 715 – 723, 2000.

Garson, G. D.: Interpreting Neural-network Connection Weights, AI Expert, 6, 46 – 51, 1991.

Goodrich, J., Campbell, D., Roulet, N., Clearwater, M., and Schipper, L.: Overriding control of methane flux temporal variability by water table dynamics in a Southern Hemisphere, raised bog, Journal of Geophysical Research: Biogeosciences, 120, 819 – 831, 2015.

Hanis, K. L., Tenuta, M., Amiro, B. D., and Papakyriakou, T. N.: Seasonal dynamics of methane emissions from a subarctic fen in the Hudson Bay Lowlands, Biogeosciences, 10, 4465 – 4479, https://doi.org/10.5194/bg-10-4465-2013, 2013.

Hashem, S.: Optimal Linear Combinations of Neural Networks., Neural networks : the official journal of the International Neural Network Society, 10, 599 – 614, https://doi.org/10.1016/S0893-6080(96)00098-6, 1997.

Hatala, J. a., Detto, M., and Baldocchi, D. D.: Gross ecosystem photosynthesis causes a diurnal pattern in methane emission from rice, Geophysical Research Letters, 39, 1 – 5, https://doi.org/10.1029/2012GL051303, 2012.

Haykin, S.: Neural Networks: a comprehensive foundation, Prentice Hall, Upper Saddle River, 1999.

Hommeltenberg, J., Mauder, M., Drösler, M., Heidbach, K., Werle, P., and Schmid, H. P.: Ecosystem scale methane fluxes in a natural temperate bog-pine forest in southern Germany, Agricultural and Forest Meteorology, 198, 273 – 284, 2014.

Hunter, A., Kennedy, L., Henry, J., and Ferguson, I.: Application of neural networks and sensitivity analysis to improved prediction of trauma survival, Computer Methods and Programs in Biomedicine, 62, 11 – 19, 2000.

Jackowicz-Korczyński, M., Christensen, T. R., Bäckstrand, K., Crill, P., Friborg, T., Mastepanov, M., and Ström, L.: Annual cycle of methane emission from a subarctic peatland, Journal of Geophysical Research, 115, 1 – 10, https://doi.org/10.1029/2008JG000913, 2010.

Jha, C. S., Rodda, S. R., Thumaty, K. C., Raha, a. K., and Dadhwal, V. K.: Eddy covariance based methane flux in Sundarbans mangroves, India, Journal of Earth System Science, 123, 1089 – 1096, https://doi.org/10.1007/s12040-014-0451-y, 2014.

Kettunen, A., Kaitala, V., Alm, J., Silvola, J., Nykänen, H., and Martikainen, P. J.: Cross-correlation analysis of the dynamics of methane emissions from a boreal peatland, Global Biogeochemical Cycles, 10, 457–471, https://doi.org/10.1029/96GB01609, 1996.

Kim, Y., Johnson, M. S., Knox, S. H., Black, T. A., Dalmagro, H. J., Kang, M., Kim, J., and Baldocchi, D.: Gap-filling approaches for eddy covariance methane fluxes: A comparison of three machine learning algorithms and a traditional method with principal component analysis, Global Change Biology, 00, 1–20, https://doi.org/10.1111/gcb.14845, 2019.

Knox, S. H., Sturtevant, C., Matthes, J. H., Koteen, L., Verfaillie, J., and Baldocchi, D.: Agricultural peatland restoration: effects of land-use change on greenhouse gas (CO_2 and CH_4) fluxes in the Sacramento-San Joaquin Delta, Global Change Biology, 21, 750 – 765, https://doi.org/10.1111/gcb.12745, 2015.

Knox, S. H., Jackson, R. B., Poulter, B., McNicol, G., Fluet-Chouinard, E., Zhang, Z., Hugelius, G., Bousquet, P., Canadell, J. G., Saunois, M., Papale, D., Chu, H., Keenan, T. F., Baldocchi, D., Torn, M. S., Mammarella, I., Trotta, C., Aurela, M., Bohrer, G., Campbell, D. I., Cescatti, A., Chamberlain, S., Chen, J., Chen, W., Dengel, S., Desai, A. R., Euskirchen, E., Friborg, T., Gasbarra, D., Goded, I., Goeckede, M., Heimann, M., Helbig, M., Hirano, T., Hollinger, D. Y., Iwata, H., Kang, M., Klatt, J., Krauss, K. W., Kutzbach, L., Lohila, A., Mitra, B., Morin, T. H., Nilsson, M. B., Niu, S., Noormets, A., Oechel, W. C., Peichl, M., Peltola, O., Reba, M. L., Richardson, A. D., Runkle, B. R. K., Ryu, Y., Sachs, T., Schäfer, K. V. R., Schmid, H. P., Shurpali, N., Sonnentag, O., Tang, A. C. I., Ueyama, M., Vargas, R., Vesala, T., Ward, E. J., Windham-Myers, L., Wohlfahrt, G., and Zona, D.: FLUXNET-CH4 Synthesis Activity: Objectives, Observations, and Future Directions, Bulletin of the American Meteorological Society, 100, 2607–2632, https://doi.org/10.1175/BAMS-D-18-0268.1, 2019.

Kroon, P. S., Schrier-Uijl, a. P., Hensen, a., Veenendaal, E. M., and Jonker, H. J. J.: Annual balances of CH4 and N2O from a managed fen meadow using eddy covariance flux measurements, European Journal of Soil Science, 61, 773 – 784, https://doi.org/10.1111/j.1365-2389.2010.01273.x, 2010.

Long, K., Flanagan, L. B., and Cai, T.: Diurnal and seasonal variation in methane emissions in a northern Canadian peatland measured by eddy covariance, Global Change Biology, 16, 2420 – 2435, https://doi.org/10.1111/j.1365-2486.2009.02083.x, 2010.

Mikhaylov, O. A., Miglovets, M. N., and Zagirova, S. V.: Vertical methane fluxes in mesooligotrophic boreal peatland in European Northeast Russia, Contemporary Problems of Ecology, 8, 368 – 375, https://doi.org/10.1134/S1995425515030099, 2015.

Naftaly, U., Intrator, N., and Horn, D.: Optimal ensemble averaging of neural networks, Network: Computation in Neural Systems, 8, 283 – 296, https://doi.org/10.1088/0954-898X/8/3/004, 1997.

Nemitz, E., Mannarella, I., Ibrom, A., Aurela, M., Burba, G. G., Dengel, S., Gielen, B., Grelle, A., Heinesch, B., Herbst, M., et al.: Standardisation of eddy-covariance flux measurements of methane and nitrous oxide, International agrophysics, 32, 517–549, 2018.

Olden, D. A. and Jackson, J. D. Y.: Illuminating the "black box": a ramdomization approach for understanding variable contributions in artificial neuronal networks., Ecological Modelling, 154, 135 – 150, 2002.

Papale, D. and Valentini, R.: A new assessment of European forests carbon exchanges by eddy fluxes and artificial neural network spatialization, Global Change Biology, 9, 525 – 535, https://doi.org/10.1046/j.1365-2486.2003.00609.x, 2003.

Parmentier, F. J. W., Van Huissteden, J., Van Der Molen, M. K., Schaepman-Strub, G., Karsanaev, S. a., Maximov, T. C., and Dolman, a. J.: Spatial and temporal dynamics in eddy covariance observations of methane fluxes at a tundra site in northeastern Siberia, Journal of Geophysical Research: Biogeosciences, 116, 1 – 14, https://doi.org/10.1029/2010JG001637, 2011.

Perrone, M. P. and Cooper, L. N.: When networks disagree: ensemble methods for hybrid neural network, in: Neural Networks for Speech and Image Processing, edited by Mammone, R. J., pp. 126 – 142, Chapman Hall, London, 1993.

Pypker, T. G., Moore, P. a., Waddington, J. M., Hribljan, J. a., and Chimner, R. C.: Shifting environmental controls on CH4 fluxes in a sub-boreal peatland, Biogeosciences, 10, 7971 – 7981, https://doi.org/10.5194/bg-10-7971-2013, 2013.

Rinne, J., Riutta, T., Pihlatie, M., Aurela, M., Haapanala, S., Tuovinen, J. P., Tuittila, E. S., and Vesala, T.: Annual cycle of methane emission from a boreal fen measured by the eddy covariance technique, Tellus, Series B: Chemical and Physical Meteorology, 59, 449 – 457, https://doi.org/10.1111/j.1600-0889.2007.00261.x, 2007.

Sarle, W. S.: Neural Networks and Statistical Models, in: Proceedings of the Nineteenth Annual SAS Users Group International Conference, April, 1994, pp. 1 – 13, https://doi.org/10.1.1.27.699, 1994.

Sarle, W. S.: Neural Network FAQ, periodic posting to the Usenet newsgroup comp.ai.neural-nets, ftp://ftp.sas.com/pub/neural/FAQ.html, 1997.

Schmidt, A., Wrzesinsky, T., and Klemm, O.: Gap Filling and Quality Assessment of CO2 and Water Vapour Fluxes above an Urban Area with Radial Basis Function Neural Networks, Boundary-Layer Meteorology, 126, 389 – 413, https://doi.org/10.1007/s10546-007-9249-7, 2008.

Shoemaker, W. B., Anderson, F., Barr, J. G., Graham, S. L., and Botkin, D. B.: Carbon exchange between the atmosphere and subtropical forested cypress and pine wetlands, Biogeosciences, 12, 2285 – 2300, https://doi.org/10.5194/bg-12-2285-2015, 2015.

Suyker, A. E., Verma, S. B., Clement, R. J., and Billesbach, D. P.: Methane flux in a boreal fen: Season-long measurement by eddy correlation, Journal of Geophysical Research: Atmospheres, 101, 28 637 – 28 647, https://doi.org/10.1029/96JD02751, 1996.

Wille, C., Kutzbach, L., Sachs, T., Wagner, D., and Pfeiffer, E.-M.: Methane emission from Siberian arctic polygonal tundra: eddy covariance measurements and modeling, Global Change Biology, 14, 1395 – 1408, https://doi.org/10.1111/j.1365-2486.2008.01586.x, 2008.

Wolpert, D. H.: Stacked generalization, Neural Networks, 5, 241 – 259, https://doi.org/10.1016/S0893-6080(05)80023-1, 1992.